Journal of Materials Chemistry B

ROYAL SOCIETY OF CHEMISTRY

PAPER

View Article Online
View Journal | View Issue

Cite this: J. Mater. Chem. B, 2022, 10, 3501

Responsive hydrogel-based microneedle dressing for diabetic wound healing†

Zhaoyang Guo,‡[a] Haiyang Liu,‡[a] Zhekun Shi,[a] Lulu Lin,[b] Yinping Li,[b] Miao Wang,*[c] Guoqing Pan,[c] Yifeng Lei*[ad] and Longjian Xue[a]

Received 17th January 2022,
Accepted 30th March 2022

DOI: 10.1039/d2tb00126h

rsc.li/materials-b

Wound healing is a critical challenge in diabetic patients, mainly due to long-term dysglycemia and its related pathological complications. Subcutaneous insulin injection represents a typical clinical solution, while the low controllability of insulin administration commonly leads to a result far from the optimal therapeutic effect. In this work, we developed a glucose-responsive insulin-releasing hydrogel for microneedle dressing fabrication and then investigated its effects on diabetic wound healing. The hydrogel system was composed of biocompatible gelatin methacrylate (GelMa), glucose-responsive monomer 4-(2-acrylamidoethylcarbamoyl)-3-fluorophenylboronic acid (AFPBA) and gluconic insulin (G-insulin), and the Gel–AFPBA–ins hydrogel-based microneedle dressing was developed by replicating PDMS molds. The resultant hydrogel microneedle dressing exhibited adequate mechanical properties, high biocompatibility, glucose-responsive insulin release behavior upon exposure to different glucose solutions, and potent adhesion to the skin compared to hydrogels without microstructures. The microneedle dressing could accelerate the diabetic wound healing process with decreased inflammatory reaction, enhanced collagen deposition on the regenerated tissue sites, and improved blood glucose control in animals. Therefore, the glucose-responsive insulin-releasing hydrogel microneedle dressing is effective in diabetic wound management and has potential for treatment of other chronic skin injuries.

1. Introduction

Diabetes is a chronic condition challenging global health, with 537 million adults living with this disease worldwide according to the latest report of the International Diabetes Federation in 2021.[1] Diabetes is associated with serious complications such as cardiovascular disease, nerve damage, kidney damage, lower-limb amputation, and eye disease. Among them, delayed wound healing and chronic wound infection are important health concerns faced by diabetic patients and improvement in their treatment is highly desired.[2–4]

Traditional treatments of diabetic wounds involve rigorous glucose control and careful wound care.[3] In addition, novel modalities that deliver natural or synthesized therapeutics, such as growth factors, primary cells or cellular products, are promising for diabetic wound repair.[5] To date, wound dressings with therapeutics have been widely employed to accelerate the healing of diabetic wounds,[5,6] since they can provide a humid environment, protect the wound from secondary infection, remove the wound exudate and promote tissue regeneration.[6,7] Dressing materials, including natural and synthetic polymers, were used in the form of films, foams, hydrocolloids and hydrogels as medicated systems *via* the delivery of encapsulated therapeutics.[8] Among them, smart hydrogels[9,10] with desired functions[11,12] or with stimulus-responsive abilities[13] have attracted great attention for diabetic wound healing. For instance, hyaluronic acid- and chitosan-based hydrogels accelerated diabetic wound healing due to the codelivery of curcumin and epidermal growth factor (EGF) with on-demand drug release.[14]

Insulin is a peptide hormone that is critical for the regulation of blood glucose (BG) levels in diabetic patients.[15] Recently, insulin has also been proven to be a potent stimulator of wound healing beyond its BG lowering action.[16] Comparably, insulin has a significantly lower cost than alternative therapeutic growth factors. Moreover, compared to the burst release of insulin, glucose-responsive insulin-releasing systems are advantageous in the regulation of BG levels in diabetic patients.[17,18] Therefore, a smart hydrogel system integrating glucose-responsive insulin-releasing behavior is promising for BG control and wound healing in diabetic patients.

[a] School of Power and Mechanical Engineering & The Institute of Technological Science, Wuhan University, Wuhan 430072, China. E-mail: yifenglei@whu.edu.cn
[b] School of Basic Medical Sciences, Wuhan University, Wuhan 430071, China
[c] Institute for Advanced Materials, School of Materials Science and Engineering, Jiangsu University, Zhenjiang 212013, China. E-mail: wangmiao@ujs.edu.cn
[d] Wuhan University Shenzhen Research Institute, Shenzhen 518057, China

† Electronic supplementary information (ESI) available. See DOI: 10.1039/d2tb00126h

‡ These authors contributed equally to this work.

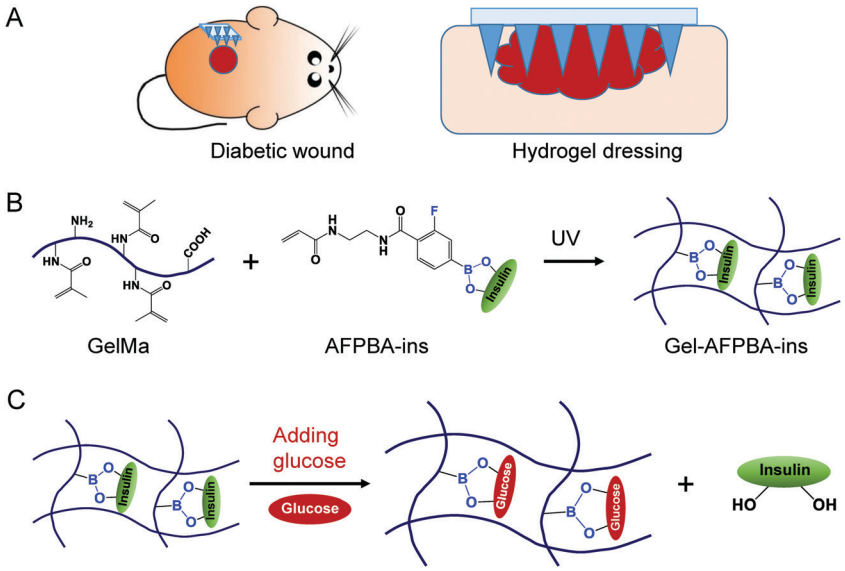

Scheme 1 Responsive microneedle dressing for diabetic wound healing. (A) Diabetic wounds in mice treated with the hydrogel-based microneedle dressing. (B) Preparation of glucose-responsive insulin-releasing Gel–AFPBA–ins hydrogels. (C) Mechanism of glucose-responsive insulin release from the prepared hydrogels.

In addition, micro/nanoscale structures on materials have attracted great interest in the field of drug delivery due to their enhancement in skin adhesiveness.[19] For example, bioinspired nanoarrays on silicone exhibited great adhesion to heart tissue;[20] moreover, bioinspired microneedle arrays provided mechanical interlocking and enhanced tissue adhesion,[21–23] therefore enhancing surgical closure and wound healing.[24–30]

Based on the above considerations, in this work, we aim to develop a glucose-responsive insulin-releasing hydrogel microneedle dressing for diabetic wound repair (Scheme 1A). The hydrogel was prepared through *in situ* copolymerization of biocompatible gelatin methacrylate (GelMa), glucose-responsive monomer 4-(2-acrylamidoethylcarbamoyl)-3-fluorophenylboronic acid (AFPBA) and gluconic insulin (G-insulin). The microneedle structure was designed to enhance the adhesion of the hydrogel to diabetic wounds (Scheme 1A), while the prepared hydrogel with phenylboronic acid (PBA) groups exhibited glucose-responsive insulin-releasing behavior (Scheme 1B and C). Together, this hydrogel-based microneedle dressing was able to accelerate wound healing through responsive insulin release and glucose control in diabetic patients.

2. Materials and methods

2.1. Materials

Gelatin methacrylate (GelMa) and lithium phenyl-2,4,6-trimethylbenzoylphosphinate (LAP) were obtained from Suzhou Intelligent Manufacturing Research Institute, China. The glucose-responsive monomer 4-(2-acrylamidoethylcarbamoyl)-3-fluorophenylboronic acid (AFPBA) was synthesized according to our previous method (Fig. S1, ESI†).[31–33] Bovine insulin was purchased from Shanghai Yuanye Bio-Technology. Glucose was obtained from Sigma–Aldrich. Phosphate buffered solution (PBS, pH ~ 7.2) was obtained from Biosharp, Hefei, China. Milli-Q water with a resistivity of 18 MΩ cm at 25 °C was used during the study.

2.2. Preparation of glucose-responsive insulin-releasing hydrogels

First, gluconic acid-modified insulin (G-insulin) was prepared according to our previous method.[17,18] Next, 1 volume of G-insulin (30 mM) was added to 1 volume of AFPBA solution (100 mM), and the mixture was reacted at room temperature for 24 h to graft G-insulin onto the end of the AFPBA molecule to obtain the AFPBA–ins complex (Fig. S2, ESI†). The obtained product was washed twice in water and ultracentrifuged with a cutoff tube (MWCO 3000, Millipore) to remove the unreacted molecules.

GelMa powder (1–10 wt%) was dissolved in water with bath sonication at 37 °C for 30 min. The photoinitiator, LAP (0.005–0.05 wt%), was then dissolved in GelMa solution, and the mixture was protected in a dark environment to prevent the crosslinking of GelMa. The obtained GelMa solution (10 wt%) and the AFPBA–ins solution were mixed at a 1 : 1 volume ratio, poured into a disk-shaped mold (with a diameter of 4 mm and a depth of 0.5 mm), and then cross-linked under UV light irradiation (365 nm) for 3 min (Scheme 1B). The obtained hydrogels with copolymerization of glucose-responsive released insulin (AFPBA–ins) were labeled Gel–AFPBA–ins (Scheme 1B). Afterwards, the resulting hydrogels were washed with PBS to remove the unreacted reagents. The insulin concentrations before the reaction and in the washing solution were measured using a Bradford Protein Assay Kit (Beyotime, China), and the amount of loaded insulin in the obtained hydrogels was calculated by subtraction. The hydrogels were fully soaked in PBS solution before use. The GelMa hydrogels without drug

loading were labeled Gel-blk. In addition, for the preparation of the control of Gel–ins group, pristine insulin was dissolved and uniformly mixed in the GelMa solution; during the photocrosslinking process of GelMa, insulin was physically embedded into the crosslinked GelMa hydrogel networks.

2.3. Preparation of hydrogel-based microneedle dressing

To enhance the adhesion of the hydrogels to wound sites, the hydrogels were further prepared in microneedle arrays by replicating PDMS molds (Fig. 4A). In brief, the above pregel solution (100 μL) was pipetted onto the surface of the PDMS mold (containing an 11 × 11 array of conical needles, each with a height of 600 μm and a base diameter of 300 μm).[34,35] The solution was uniformly filled into the mold cavity under vacuum for 3 minutes to form needle tips, and then the solution was removed from the mold surface. Next, a self-made fence is fixed on the top surface of the PDMS mold, and the solution is filled into the fence. Then, the solution was cross-linked under UV light irradiation (Fig. 4A). The microneedle arrays were dried at room temperature overnight and peeled off from the PDMS molds for subsequent use.

2.4. Physical–chemical characterization

X-ray photoelectron spectroscopy (XPS, Thermo Fisher ESCALAB 250Xi) and Fourier transform infrared spectroscopy (FTIR, Thermo Fisher FTIR5700) were used to analyze the elemental composition and chemical structure of the obtained hydrogels, respectively. A high-resolution camera of a cell phone (Redmi K30) and scanning electron microscope (SEM; Tescan Mira3) were used to visualize the appearance and cross-sectional morphology of the samples, respectively.

2.5. Adhesion force measurement

The adhesive properties of the hydrogels and microneedle dressings were evaluated using a universal testing machine (Shenzhen Suns Technology, UTM2503) in tensile mode. Briefly, a piece of 2 wt% agarose gel was prepared to mimic the skin-like tissue surface and fixed on the bottom platform of the tensile testing machine using double faced adhesive tape (Fig. 4C). Meanwhile, the samples, including the hydrogels and the microneedle dressings (1 cm × 1 cm), were fixed on the top platform of the machine (Fig. 4C). The samples were allowed to attach to the surface of the agarose gel under a gentle finger press for 1 minute. Then, the top platform with the samples was slowly lifted until the separation of the samples from skin-like surfaces (Fig. 4C). The maximum force at the moment of separation was recorded, and the adhesive stress of the samples was calculated accordingly.

2.6. *In vitro* drug release assay

The drug release from the hydrogels was performed in different glucose solutions, including 100 mg dL^{-1} and 400 mg dL^{-1} glucose solutions, which represent the physiological levels of BG from healthy to diabetic subjects, respectively. The samples were incubated in 1000 μL glucose solutions at 37 °C. At different time points, 5 μL of the supernatant was collected, and 5 μL of glucose solution was replenished into the well. The concentration of released insulin in the supernatant was measured through the Bradford Protein Assay Kit. Then, the accumulated insulin release from the hydrogels was plotted as a function of incubation time.

2.7. Cell culture study

Mouse fibroblast L929 cells were cultured in RIPM 1640 medium (Gibco) with 10% fetal bovine serum (FBS, HyClone) and 1% penicillin–streptomycin (PS, HyClone). The compatibility of the hydrogels with the cells was evaluated by the CCK-8 test. In brief, the hydrogels were incubated with 0.2 g mL^{-1} culture medium and shaken at 37 °C for 24 h. The extract was collected after filtration. Cell culture medium without any treatment was used as the control medium. L929 cells were seeded in 96-well plates at a density of 2000 cells per well (n = 5 for each group). After cell adhesion to the plate for 24 h, the cell culture medium was replaced with 200 μL of extract medium or control medium and incubated for 24 h, 48 h and 72 h, respectively. At different time points, the cell viability was evaluated using a CCK-8 assay kit (Dojindo, Japan) according to the manufacturer's instructions.

2.8. Animal study

2.8.1. Animal model. All animal experiments were approved by the Institutional Animal Care and Use Committee (IACUC No. WP20210398) of Wuhan University. C57BL/6 mice (8 weeks, male) were obtained from Beijing SPF Biotechnology (China) and raised in a specific pathogen free environment. According to our previous methods,[17,34–36] insulin-dependent diabetes, known as type 1 diabetes, was induced through five intraperitoneal injections of streptozotocin (STZ, Sigma–Aldrich) into the mice. When the BG levels were higher than 16 mM, the diabetic mouse model was ready for the next experimental use.

2.8.2. Skin adhesive test. The adhesive ability of the samples on the skin of mice was evaluated by a peeling test. Briefly, a hydrogel slice (1 cm × 1 cm) or a microneedle dressing (1 cm × 1 cm) was attached onto the surface of the mouse skin, and compressed gently with a finger using the same force for 30 seconds. Afterwards, the samples were peeled from the skin surface, and the peeling process was recorded using a cell phone (Redmi K30).

2.8.3. Diabetic wound healing test. Diabetic mice were anesthetized by intraperitoneal injection of 1% sodium pentobarbital (Sigma-Aldrich). The dorsal regions of the mice were shaved and cleaned. A round wound was generated on the shaved skin using biopsy punches (5 mm diameter). Then the wounds were applied with different microneedle dressings, including Gel-blk, Gel–ins, Gel–AFPBA–ins, and the untreated wound as the control group (n = 7 per group). In brief, the dorsum skin of mice was folded, the microneedle patch was attached on one side of the folded skin with the wound, and the substrate of the patch was thumb-pressed for 30 seconds. Afterward, the breathable medical adhesive membrane (Hons Medical, China) was applied to fix the samples in place. One piece of microneedle dressing was applied onto the mouse

wound once per day, and changed over 8 days. For the analgesia, the mice with a dorsal wound received meloxicam with subcutaneous injection at a dose of 2 mg kg^{-1} every 24 hours. The mice with wound were individually raised in each cage. The BG levels of the mice were recorded daily, and the wounds were photographed daily using a cell phone. The wound areas were analyzed using ImageJ software (NIH, USA).

After 8 days of treatment, the mice were euthanized, and the skin tissues surrounding the wounds were excised and fixed in 4% paraformaldehyde for histological analysis. Tissues were sectioned and stained with an H&E staining kit and Masson's trichrome staining kit. The stained samples were scanned using a Pannoramic Scan system (3DHISTECH) and analyzed using CaseViewer software (3DHISTECH).

2.9. Statistical analysis

Data are presented as the mean value ± standard deviation (s.d.). *In vitro* experimental results were acquired by at least five samples for three repetitions. *In vivo* results were obtained by averaged analysis of seven mice per group. The histological analysis was summarized based on at least three random images in each section and three sections per animal. The statistical significance was determined using Student's *t* test (OriginPro® 2021, OriginLab), and a *p* value less than 0.05 was considered significantly different.

3. Results

3.1. Preparation of Gel–AFPBA–ins hydrogels

We prepared Gel–AFPBA–ins hydrogels using GelMa and AFPBA–ins (Scheme 1B). GelMa was employed as a scaffold hydrogel due to its good biocompatibility, controllable mechanical properties, and most importantly, photocrosslinking ability due to the acrylamide group,[37] and broad biomedical applications.[38,39] Meanwhile, the AFPBA–ins complex can be functionalized onto the GelMa scaffold because of its photocrosslinking property (Scheme 1B), in which the AFPBA molecule is responsible for the reaction with glucose and release of insulin (Scheme 1C). The AFPBA molecule had a pK_a of 7.2,[40] which was slightly lower than physiological pH (7.4), allowing interaction with diols and glucose sensitivity under physiological conditions.[31–33]

First, we investigated the crosslinking ability of different concentrations of GelMa. When the concentration of GelMa was less than 5 wt%, it was difficult for the solution to form a gel (Fig. S3, ESI†). As the concentration of GelMa increased, the GelMa solution rapidly cross-linked into gels (Fig. S3, ESI†), and the obtained hydrogels exhibited good mechanical properties for convenient handling. However, higher concentrations of GelMa increased the crosslinking density, therefore hampering the future expansion of hydrogels. To balance the good mechanical properties and maximum hydrogel expansion with glucose responsiveness, 5 wt% GelMa was selected to prepare Gel–AFPBA–ins hydrogels. With this concentration, each piece of Gel–AFPBA–ins hydrogel contained approximately 35 nmol insulin after the washing process.

3.2. Characterization of hydrogels

We employed FTIR to investigate the chemical structures and composition of hydrogels with different modifications (Fig. 1A and Fig. S4, ESI†). For pristine GelMa in which gelatin protein was functionalized with methacrylate,[37] two wide shoulders appeared, including 1628 cm^{-1} related to C=O stretching (amide I band) and 1538 cm^{-1} for N–H bending (amide II band) (Fig. 1A), which corresponded to typical characteristics of the protein backbone.[41] Moreover, 1232 cm^{-1} related to C–N stretching plus N–H bending (Fig. 1A),[42] 3284 cm^{-1} to N–H stretching (amide A), 3072 cm^{-1} to sp^2 C–H stretching, and 2391 cm^{-1} to sp^3 C–H stretching (Fig. S4, ESI†) appeared, and these peaks confirmed the chemical structures of GelMa.

For the AFPBA molecule, typical IR peaks of the molecule existed, including peaks at 3478 cm^{-1} for O–H stretching (Fig. S4, ESI†), 1413 cm^{-1} for benzene ring bonding, 1348 and 1045 cm^{-1} for B–O bonding, 1250 and 1100 cm^{-1} for C–B bonding,[43] 1145 cm^{-1} for C–F bonding, and 804, 771 and 704 cm^{-1} for *para*, *ortho* and *meta* aromatic sp^2 C–H bending,[44] respectively (Fig. 1A).

For AFPBA–ins in which AFPBA was grafted with G-insulin (Fig. S2, ESI†), the type IR peaks of protein existed, whereas the

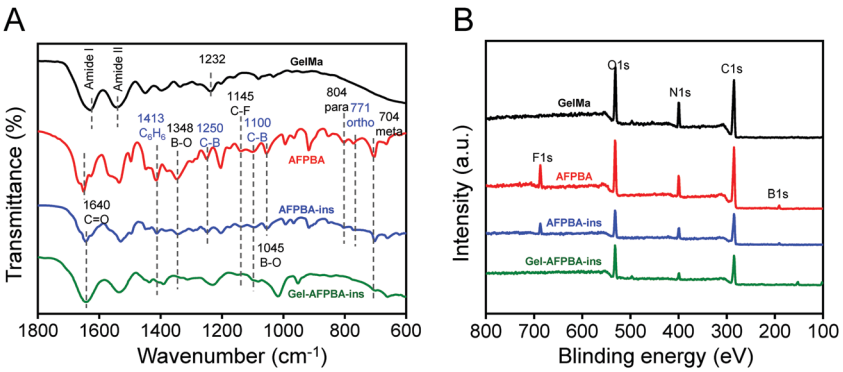

Fig. 1 FTIR and XPS analysis of glucose-responsive insulin-releasing hydrogels. (A) FTIR spectra from 1800 to 600 cm^{-1}, and (B) XPS wide spectra during the preparation of hydrogels.

typical peaks from the AFPBA molecule slightly decreased (Fig. 1A), indicating the combination of AFPBA with G-insulin.

With further conjugation of GelMa with the AFPBA–Ins complex to form Gel–AFPBA–ins (Scheme 1B), the type IR peaks of the protein still existed, whereas the typical peaks from the AFPBA molecule further decreased (Fig. 1A). However, the IR peaks from AFPBA–ins, including C_6H_6 at 1413 cm^{-1}, B–O at 1384 cm^{-1}, C–B at 1100 cm^{-1}, and *meta* aromatic C–H bending at 704 cm^{-1}, still existed in Gel–AFPBA–ins (Fig. 1A), revealing the successful formation of Gel–AFPBA–ins by the combination of GelMa and AFPBA–ins.

In addition, we performed XPS analysis to evaluate the changes in elemental positions during different modifications. Compared to GelMa which showed typical peaks of C, N and O elements, AFPBA showed significant contents of B and F (Fig. 1B and Fig. S5, ESI†). Meanwhile, AFPBA–ins exhibited a decreased amount of B and F (Fig. 1B and Fig. S5, ESI†) due to the presence of AFPBA molecule on G-insulin. Gel–AFPBA–Ins hydrogels showed a further decrease in the content in B and F (Fig. 1B and Fig. S5, ESI†), which was derived from the AFPBA–ins molecule.

3.3. *In vitro* swelling

We chose to integrate the glucose-sensitive molecule AFPBA into the hydrogel scaffold due to the suitable equilibrium associate constant of the molecule with glucose (Scheme 1B).[31,32] Meanwhile, G-insulin was used instead of pristine insulin (Scheme 1B and Fig. S2, ESI†) to achieve glucose-responsive insulin releasing behavior of the hydrogels (Scheme 1C), taking advantage that the end of AFPBA combines reversibly with *cis*-diol units on glucose.[45,46]

After photocrosslinking, the obtained hydrogels were transparent in appearance (Fig. S3, ESI†), with a diameter of 4 mm and a surface area of 12.57 mm^2. After reaction with different glucose solutions, the morphological changes and expansion in hydrogels were not visible compared to the as-prepared hydrogels (Fig. 2A, insert), with surface areas of 12.13 mm^2, 12.87 mm^2, and 13.17 mm^2, respectively (Fig. 2B). In detail, the swelling of Gel–AFPBA–ins hydrogels slightly increased from a lower glucose concentration (0 or 100 mg dL^{-1}) to a concentrated glucose solution (400 mg dL^{-1}) (Fig. 2B). The swelling degree was further confirmed by SEM observation of the freeze-dried cross-sections of the hydrogels. After immersion in PBS solution, the Gel–AFPBA–ins hydrogel showed a porous structure with an average pore size of 1.77 ± 0.31 μm (Fig. 2A and C). After immersion into glucose solutions, the pore size of the hydrogels increased, and the higher the glucose concentrations were, the larger the pore sizes of the hydrogels (Fig. 2A and C). The variation in the pore size of the hydrogels was consistent with their changes in morphological expansion (Fig. 2B and C). After immersion in glucose solutions, glucose molecules diffused into the hydrogels. The anionic boronate species of the hydrogels had a substantial affinity and preferred binding to the diols of glucose molecules to form cyclic boranate esters (Scheme 1C). The formation of boronate anions increased the Donnan osmotic pressure of the hydrogels,[47–49] resulting in an expansion of the hydrogels.

3.4. *In vitro* drug release

We also evaluated the insulin release kinetics from the hydrogels in response to different glucose concentrations. The insulin release was rapid and almost completed within 150 min (Fig. 2D), which is within the time frame of normal insulin secretion in the body.[15] The drug release profile was found to be dependent on glucose concentrations. In the hyperglycemic environment (400 mg dL^{-1}), faster and more insulin release was achieved from the hydrogels (Fig. 2D). In contrast, relatively slower and less insulin was released from the hydrogels when immersed in normal glucose levels (100 mg dL^{-1}) and glucose free PBS solution (Fig. 2D). The drug release profile was

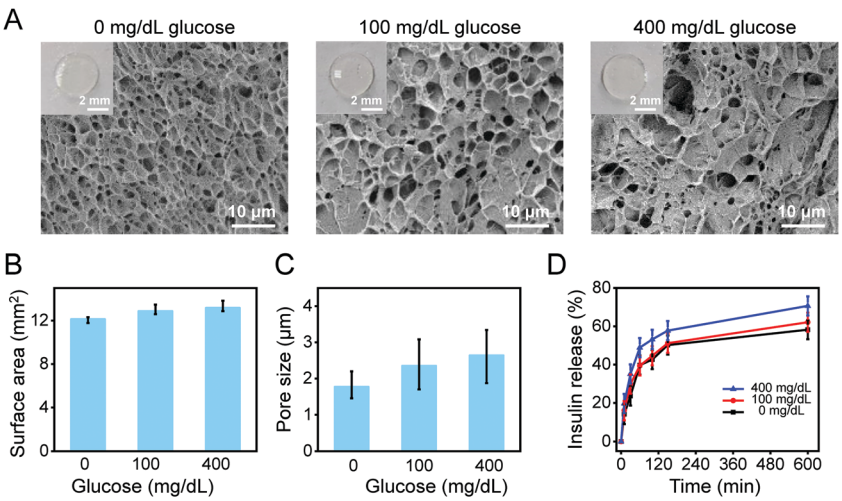

Fig. 2 Glucose responsiveness and insulin release of the Gel–AFPBA–ins hydrogels. (A) SEM images of the cross-sectional morphology of the hydrogels after reaction with different glucose solutions. The insets show the appearance of the corresponding hydrogels. (B) Surface area and (C) average pore size of the hydrogels after reaction with different glucose solutions. (D) Insulin release kinetics from the hydrogels in different glucose solutions. Mean ± s.d. (n = 5 for 3 repetitions).

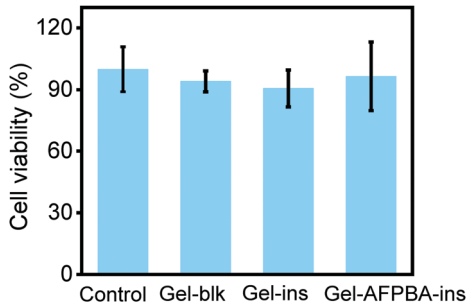

Fig. 3 Cell viability of the hydrogels in different formulations. Cell culture medium without any treatments served as the control. Mean ± s.d. (n = 5 for 3 repetitions).

consistent with the above swelling response of the hydrogels (Fig. 2A–C). The copolymerization of AFPBA in the hydrogels not only provided a volumetric response to glucose but also endowed the hydrogels with responsive release kinetics of insulin. As described above, the boronate species of AFPBA preferred binding to the diols group of glucose,[49] and this reaction triggered the Gel–AFPBA–ins hydrogels to release G-insulin in the presence of glucose (Scheme 1C). The higher the glucose concentrations were, the more glucose molecules competed with the boronate species (Scheme 1C); therefore more insulin was released from the hydrogels (Fig. 2D). These results indicate that the hydrogel dressing can respond to physiological levels of glucose concentrations and release insulin upon glucose levels.

3.5. *In vitro* cytotoxicity

We evaluated the cell biocompatibility of the hydrogels using mouse L929 fibroblast cells. Different hydrogels were incubated with cell culture medium at 37 °C for 24 h and were later collected for cell culture after filtration. A CCK-8 assay was performed to evaluate the metabolic activity of L929 cells treated with different hydrogels. For all groups, including Gel-blk, Gel–ins and Gel–AFPBA–ins hydrogels, the cell viability was higher than 90% after 72 h of incubation, and there was no significant difference between the Gel–AFPBA–ins group and the control group (Fig. 3). This result indicated negligible cytotoxicity of the hydrogels toward L929 cells.

3.6. Hydrogel-based microneedle dressing

Strong tissue adhesion is highly required for many biomedical applications including wound closure and fixing implantable devices.[50,51] To enhance the adhesion of the hydrogels with the skin tissues, the above hydrogels in the architecture of the microneedle dressing were developed (Fig. 4A). The fabricated microneedle dressing was well arranged in an array of 11 × 11 needles, which exhibited a conical shape with slight deformation in the tips (Fig. 4B). The adhesion strength of the microneedle dressing to the skin-like surface was measured by tensile testing (Fig. 4C).[52] Compared to the hydrogels without any microarchitecture, the hydrogel-based microneedle dressing showed an improvement of 47% in the adhesion strength to the skin-like surface (Fig. 4D, $p < 0.01$). Moreover, the adhesion and peeling test on the mouse skin showed that the hydrogels without microstructure could be easily removed from the skin of mice (Fig. 4E). However, after adhesion to the skin, peeling of the microneedle dressing from the skin was relatively difficult (Fig. 4F). These results demonstrated that the microneedle dressing enhanced the adhesion of hydrogels to the skin, mainly due to the specific microstructure of the

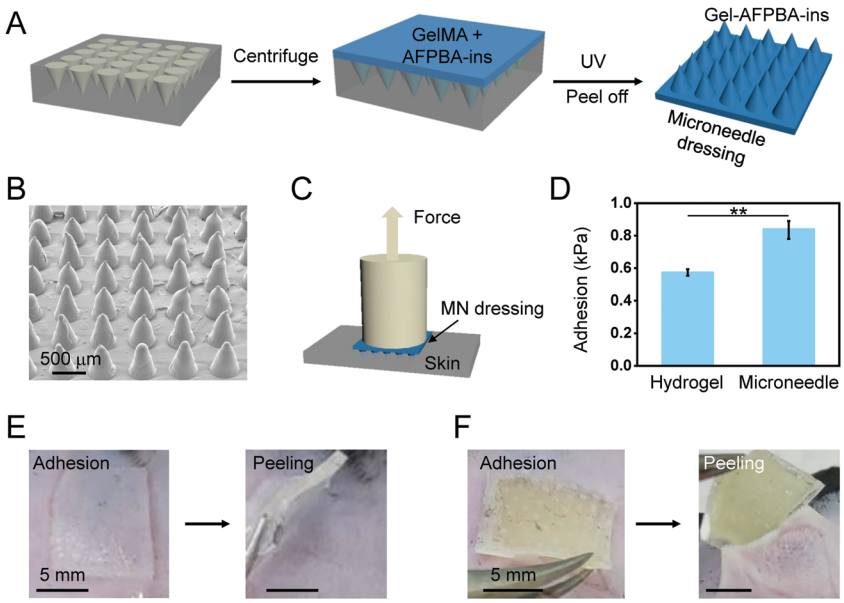

Fig. 4 Preparation and characterization of the adhesion force of the hydrogel-based microneedle dressing. (A) Preparation process of the microneedle dressing. (B) SEM image of the prepared microneedle dressing. (C) Schematic illustration of the adhesion force test. (D) Adhesion strength of the samples. Mean ± s.d. (n = 5). (E) Images of adhesion and peeling of the hydrogel dressing from the mouse skin. (F) Adhesion and peeling of the microneedle dressing from the mouse skin. ** $p < 0.01$.

microneedles, which increased the relative areas and roughness of the surfaces (Fig. 4B).[52,53]

3.7. *In vivo* wound healing

We examined the efficacy of the above hydrogel-based microneedle dressing for wound healing in STZ-induced diabetic mice. The diabetic wounds were evenly divided into four groups, including wounds without any dressing treatment (Control), wounds treated with blank GelMa hydrogels without insulin loading (Gel-blk), GelMa hydrogels loaded with insulin with physical absorption (Gel–ins), and Gel–AFPBA–ins hydrogels in the form of a microneedle dressing. As time went on, diabetic wound areas gradually decreased in all groups (Fig. 5A and B), indicating wound closure. After 8 days, the wound areas decreased by 71.6% and 62.8% in the Control and Gel-blk groups, respectively (Fig. 5B). Comparably, wound healing in the Gel–ins and Gel–AFPBA–ins groups was more significant (Fig. 5A). More specifically, the wound healing was faster in the Gel–AFPBA–ins group (Fig. 5A), with 89.3% of the wound area healed after 8 days of treatment (Fig. 5B). And the wound areas treated with Gel–AFPBA–ins were significantly smaller than other groups (Fig. 5B, $p < 0.05$ or $p < 0.001$). These results proved that the wounds treated with the Gel–AFPBA–ins dressing exhibited a smaller wound area, with a higher recovery rate than the other groups. Moreover, we found that the wound healing process was correlated with BG levels in mice (Table S1, ESI†). The BG levels in mice treated with Gel–AFPBA–ins were lower than those in the other groups (Table S1, ESI†), and the improved glucose control contributed to the better wound healing process in the Gel–AFPBA–ins group.

We analyzed the wound tissues by immunohistochemical staining. During the wound healing process, the growth of granulation tissue is a reflection of the early stage of wound recovery.[3] From H&E staining, numerous granulation tissues were found in the wounds treated by the control group (Fig. 6A). The wounds in the Gel-blk and Gel–ins groups showed visible scar formation (Fig. 6A). In contrast, the wounds treated with Gel–AFPBA–ins presented a significantly lower level of inflammatory infiltration than the other groups (Fig. 6A), as demonstrated by the thinner granulation tissue at the wound site (Fig. 6C), which also indicated that the skin tissues were healed after the early stage of wound recovery. Comparably, the thickness of granulation tissues with Gel–AFPBA–ins treatment was significantly thinner than those in other groups (Fig. 6C, $p < 0.01$). In the healed wound tissues of the Gel–AFPBA–ins groups, the surface cells in the epidermis covered the wound more evenly, and the cells in the dermis were more quickly recruited (Fig. 6A), which is favorable for rebuilding blood vessels and the extracellular microenvironment in the skin during healing.

Moreover, collagen proteins are the main components of skin tissues, and collagen deposition is a key issue in the later stage of wound healing.[54] Masson's trichrome staining was performed to evaluate collagen deposition in the regenerated skin tissues. As indicated by the blue color in the wound sites, collagen fibers were abundantly deposited in the regenerated skin tissues of the wounds treated with the Gel–AFPBA–ins group (Fig. 6B). In the other groups, collagen deposition remained limited (Fig. 6B). Comparably, the amount of collagen deposition after Gel–AFPBA–ins treatment was significantly higher than that in the other groups (Fig. 6D, $p < 0.01$ or $p < 0.001$).

The above histological staining results demonstrated that the Gel–AFPBA–ins dressing facilitated the healing process of diabetic wounds by reducing inflammatory infiltration and enhancing collagen deposition.

4. Discussion

Diabetic wound healing is a complex process,[5] which involves repair of damaged tissues and restoration of skin integrity.[55] Insulin is a hormone which plays a key role in the regulation of BG levels in the body.[15] Meanwhile, insufficient insulin levels exist in diabetic skin during wound healing,[56,57] which ultimately reduces the recovery rate of diabetic wounds. Topical application of insulin has been reported as being potent to improve wound healing in diabetic animals.[56,57] In addition, glucose-responsive insulin release was advantageous in the regulation of BG levels in diabetic patients,[17,18] therefore glucose-responsive insulin-releasing dressings may be promising for BG regulation and wound healing in diabetic patients.

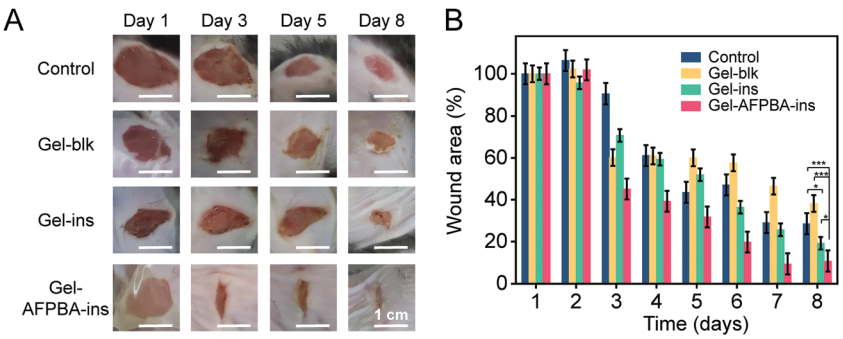

Fig. 5 Wound healing of the hydrogel-based microneedle dressing. (A) Representative images of diabetic wounds with different treatments. (B) Quantification of relative surface area of the wounds with different treatments. Wounds left undressed served as the control. Mean ± s.d. (n = 7 mice for each group). * $p < 0.05$ and *** $p < 0.001$.

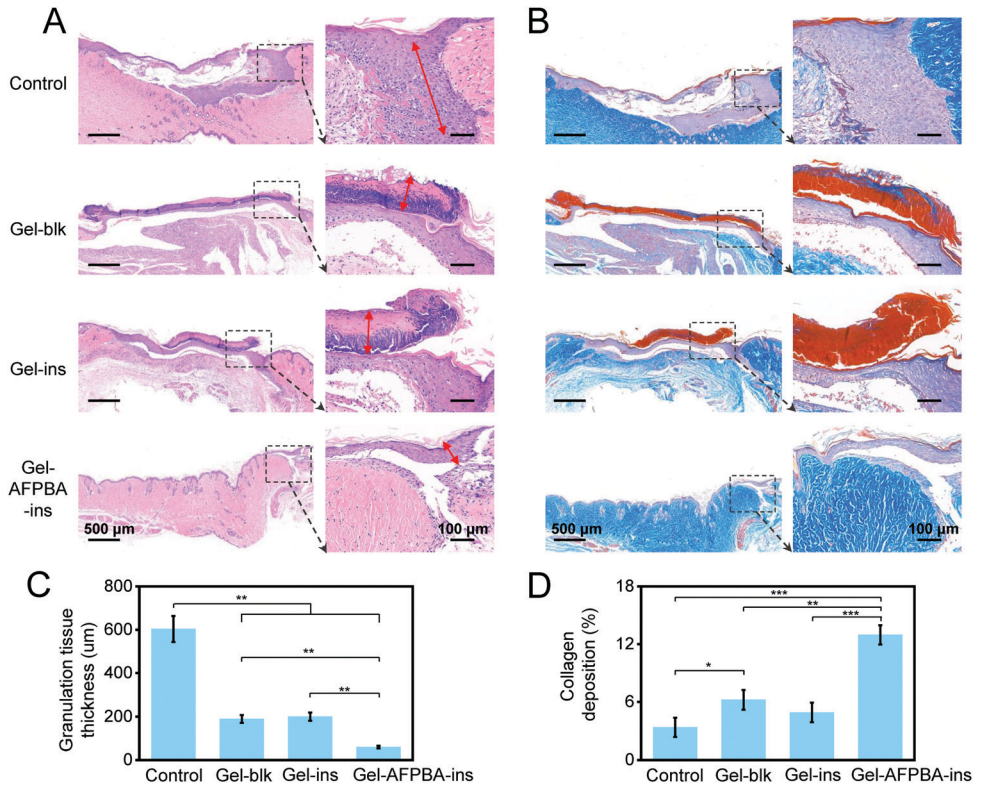

Fig. 6 Immunohistochemical analysis of the regenerated skin tissues with different treatments. (A) Images of H&E staining of the wounds. The red arrows indicate the granulation tissues. (B) Images of Masson's trichrome staining of the wounds. (C) Quantification of the thickness of granulation tissues at the wound sites. (D) Quantification of the relative amount of collagen deposition in the regenerated skin tissues. Wounds left undressed served as the control. Mean ± s.d. (n = 7 mice for each group). * $p < 0.05$, ** $p < 0.01$, and * $p < 0.001$.

In this study, we integrated a glucose-responsive insulin-releasing hydrogel (Gel–AFPBA–ins) into microneedle dressing to accelerate diabetic wound healing by utilizing the intelligent drug release on microneedle dressings (Scheme 1). The Gel–AFPBA–ins hydrogel was successfully prepared by *in situ* copolymerization of GelMa and AFPBA–ins (Scheme 1B), which was proved by XPS and FTIR analysis (Fig. 1 and Fig. S4, S5, ESI†). The prepared Gel–AFPBA–ins hydrogel had good biocompatibility toward skin cells (Fig. 3), and showed glucose-responsive insulin-releasing behavior upon exposure to different glucose solutions (Fig. 2).

Furthermore, the glucose-responsive insulin-releasing hydrogel was fabricated into a microneedle dressing in PDMS molds (Fig. 4), with the aim to enhance skin adhesion and accelerate diabetic wound healing (Scheme 1). Due to the specific microstructures, microneedle dressings possessed a fixation part which enhanced skin adhesion, played an essential role in transdermal drug delivery and promoted the process of wound healing.[24–30] Indeed, the resultant microneedle dressing exhibited adequate mechanical properties, and potent adhesion to the skin compared to hydrogels without microstructures (Fig. 4). The microneedle dressing enhanced the skin adhesion, through the increased roughness and relative area of the surfaces (Fig. 4B).[52,53]

When applied on diabetic wounds, the Gel–AFPBA–ins hydrogel microneedle dressing accelerated the wound healing process (Fig. 5), with decreased inflammatory infiltration and enhanced collagen deposition on the regenerated tissue sites (Fig. 6), and improved control of BG levels in the animals (Table S1, ESI†). Benefiting from the good biocompatibility (Fig. 3), the glucose-responsive insulin-releasing behavior (Fig. 2) and improved control of BG levels in diabetic patients (Table S1, ESI†), the hydrogel microneedle dressing promoted the cellular response to tissue injury (Fig. 6), and accelerated the wound healing process in diabetic patients (Fig. 5). The effects of topical insulin on promoting diabetic wound healing were associated with the switching of cellular signaling proteins,[58] including reduced inflammatory reactions,[56,57] the production and activation of proteases, including collagenase, and increased angiogenesis in the diabetic wound environment.[5]

Overall, we successfully developed a microneedle dressing using glucose-responsive insulin-releasing hydrogels. The microneedle dressings were multifunctional to meet the needs of skin tissue adhesion and diabetic wound repair, *via* the impaired inflammatory response and restoration of skin integrity. This hydrogel microneedle dressing is effective in diabetic wound management and has great potential for the treatment of other chronic skin injuries. Further investigations are needed to understand the molecular mechanism of the effect of glucose-responsive insulin release on the healing of type 1 diabetic wounds. In addition, the therapeutic effect of microneedle dressing on other types of diabetes can be further

investigated in future study, by utilizing specific types of diabetic models and by introducing specific medications (such as metformin). Moreover, since structural adhesion,[59] which is determined by special microstructures, is important for strong adhesion to various tissue surfaces, in the future studies, different microstructures need to be investigated to enhance tissue adhesion and wound repair.

5. Conclusions

In this work, we developed a microneedle dressing based on glucose-responsive insulin-releasing Gel–AFPBA–ins hydrogels for successful diabetic wound healing. The hydrogels were fabricated by photocrosslinking of GelMa and a glucose-responsive insulin-releasing element. The hydrogels exhibited glucose-responsive properties, as well as responsive insulin release kinetics. The Gel–AFPBA–ins hydrogels showed no apparent cytotoxicity to L929 fibroblast cells. Furthermore, the hydrogel-based microneedle dressing was fabricated by replicating PDMS molds and proved to have much stronger adhesion to skin tissues than hydrogels without microarchitectures. Furthermore, the Gel–AFPBA–ins hydrogel-based microneedle dressing accelerated the healing process of diabetic wounds by reducing inflammatory infiltration and increasing collagen deposition, as well as relatively better glucose control in diabetic patients. The microneedle dressings were biocompatible, showed glucose-responsive insulin-releasing ability, exhibited great potential for the development of substitutes for diabetic wound management, and showed potential in the treatment of chronic skin injuries.

Author contributions

Zhaoyang Guo and Haiyang Liu: data curation, formal Analysis, and investigation. Zhekun Shi and Lulu Lin: methodology. Yinping Li: resources. Miao Wang: resources and validation. Guoqing Pan: writing – review & editing. Yifeng Lei: conceptualization, funding acquisition, project administration, and writing – original draft. Longjian Xue: supervision.

Conflicts of interest

The authors declare that they have no conflicts of interest.

Acknowledgements

The authors thank the National Natural Science Foundation of China (81871484, 82172096 and 21875092) and the Guangdong Basic and Applied Basic Research Foundation (2021A1515012183) for financial support.

References

1 International Diabetes Federation. IDF Diabetes Atlas, 10th edition, 2021.
2 G. C. Gurtner, S. Werner, Y. Barrandon and M. T. Longaker, Wound repair and regeneration, *Nature*, 2008, **453**, 314–321.
3 V. Falanga, Wound healing and its impairment in the diabetic foot, *Lancet*, 2005, **366**, 1736–1743.
4 Y. Liu, S. Zeng, W. Ji, H. Yao, L. Lin, H. Cui, H. A. Santos and G. Pan, Emerging theranostic nanomaterials in diabetes and its complications, *Adv. Sci.*, 2021, **1**, 2102466.
5 S. A. Eming, P. Martin and M. Tomic-Canic, Wound repair and regeneration: mechanisms, signaling, and translation, *Sci. Transl. Med.*, 2014, **6**, 265sr266.
6 L. I. F. Moura, A. M. A. Dias, E. Carvalho and H. C. de Sousa, Recent advances on the development of wound dressings for diabetic foot ulcer treatment—A review, *Acta Biomater.*, 2013, **9**, 7093–7114.
7 D. Chouhan, N. Dey, N. Bhardwaj and B. B. Mandal, Emerging and innovative approaches for wound healing and skin regeneration: current status and advances, *Biomaterials*, 2019, **216**, 19.
8 S. Saghazadeh, C. Rinoldi, M. Schot, S. S. Kashaf, F. Sharifi, E. Jalilian, K. Nuutila, G. Giatsidis, P. Mostafalu and H. Derakhshandeh, *et al.*, Drug delivery systems and materials for wound healing applications, *Adv. Drug Delivery Rev.*, 2018, **127**, 138–166.
9 J. Koehler, F. P. Brandl and A. M. Goepferich, Hydrogel wound dressings for bioactive treatment of acute and chronic wounds, *Eur. Polym. J.*, 2018, **100**, 1–11.
10 T. Su, M. Zhang, Q. Zeng, W. Pan, Y. Huang, Y. Qian, W. Dong, X. Qi and J. Shen, Mussel-inspired agarose hydrogel scaffolds for skin tissue engineering, *Bioact. Mater.*, 2021, **6**, 579–588.
11 X. D. Zhao, D. N. Pei, Y. X. Yang, K. Xu, J. Yu, Y. C. Zhang, Q. Zhang, G. He, Y. F. Zhang and A. Li, *et al.*, Green tea derivative driven smart hydrogels with desired functions for chronic diabetic wound treatment, *Adv. Funct. Mater.*, 2021, **31**, 2009442.
12 H. Chen, R. Cheng, X. Zhao, Y. Zhang, A. Tam, Y. Yan, H. Shen, Y. S. Zhang, J. Qi and Y. Feng, *et al.*, An injectable self-healing coordinative hydrogel with antibacterial and angiogenic properties for diabetic skin wound repair, *NPG Asia Mater.*, 2019, **11**, 3.
13 M. C. Koetting, J. T. Peters, S. D. Steichen and N. A. Peppas, Stimulus-responsive hydrogels: Theory, modern advances, and applications, *Mater. Sci. Eng., R*, 2015, **93**, 1–49.
14 B. Hu, M. Gao, K. O. Boakye-Yiadom, W. Ho, W. Yu, X. Xu and X.-Q. Zhang, An intrinsically bioactive hydrogel with on-demand drug release behaviors for diabetic wound healing, *Bioact. Mater.*, 2021, **6**, 4592–4606.
15 A. R. Saltiel and C. R. Kahn, Insulin signalling and the regulation of glucose and lipid metabolism, *Nature*, 2001, **414**, 799–806.
16 M. Hrynyk and R. J. Neufeld, Insulin and wound healing, *Burns*, 2014, **40**, 1433–1446.
17 Y. Zhang, M. Wu, W. Dai, Y. Li, X. Wang, D. Tan, Z. Yang, S. Liu, L. Xue and Y. Lei, Gold nanoclusters for controlled insulin release and glucose regulation in diabetes, *Nanoscale*, 2019, **11**, 6471–6479.

18 Y. Zhang, M. Wu, W. Dai, M. Chen, Z. Guo, X. Wang, D. Tan, K. Shi, L. Xue and S. Liu, *et al.*, High drug-loading gold nanoclusters for responsive glucose control in type 1 diabetes, *J. Nanobiotechnol.*, 2019, **17**, 74.
19 Z. Ma, G. Bao and J. Li, Multifaceted Design and Emerging Applications of Tissue Adhesives, *Adv. Mater.*, 2021, **33**, e2007663.
20 Y.-C. Chen and H. Yang, Octopus-inspired assembly of nanosucker arrays for dry/wet adhesion, *ACS Nano*, 2017, **11**, 5332–5338.
21 S. Y. Yang, E. D. O'Cearbhaill, G. C. Sisk, K. M. Park, W. K. Cho, M. Villiger, B. E. Bouma, B. Pomahac and J. M. Karp, A bio-inspired swellable microneedle adhesive for mechanical interlocking with tissue, *Nat. Commun.*, 2013, **4**, 1702.
22 E. Y. Jeon, J. Lee, B. J. Kim, K. I. Joo, K. H. Kim, G. Lim and H. J. Cha, Bio-inspired swellable hydrogel-forming double-layered adhesive microneedle protein patch for regenerative internal/external surgical closure, *Biomaterials*, 2019, **222**, 119439.
23 D. Han, R. S. Morde, S. Mariani, A. A. La Mattina, E. Vignali, C. Yang, G. Barillaro and H. Lee, 4D Printing of a Bioinspired Microneedle Array with Backward-Facing Barbs for Enhanced Tissue Adhesion, *Adv. Funct. Mater.*, 2020, **30**, 1909197.
24 B. Gao, M. Guo, K. Lyu, T. Chu and B. He, Intelligent silk fibroin based microneedle dressing (i-SMD), *Adv. Funct. Mater.*, 2020, **31**, 2006839.
25 M. Guo, Y. Wang, B. Gao and B. He, Shark tooth-inspired microneedle dressing for intelligent wound management, *ACS Nano*, 2021, **15**, 15316–15327.
26 Y. Wang, H. Lu, M. Guo, J. Chu, B. Gao and B. He, Personalized and programmable microneedle dressing for promoting wound healing, *Adv. Healthcare Mater.*, 2022, **11**, 2101659.
27 X. Zhang, G. Chen, Y. Liu, L. Sun, L. Sun and Y. Zhao, Black phosphorus-loaded separable microneedles as responsive oxygen delivery carriers for wound healing, *ACS Nano*, 2020, **14**, 5901–5908.
28 J. Chi, L. Sun, L. Cai, L. Fan, C. Shao, L. Shang and Y. Zhao, Chinese herb microneedle patch for wound healing, *Bioact. Mater.*, 2021, **6**, 3507–3514.
29 L. Sun, L. Fan, F. Bian, G. Chen, Y. Wang and Y. Zhao, MXene-integrated microneedle patches with innate molecule encapsulation for wound healing, *Research*, 2021, **2021**, 9838490.
30 Y. Sun, J. L. Liu, H. Y. Wang, S. S. Li, X. T. Pan, B. L. Xu, H. L. Yang, Q. Y. Wu, W. X. Li and X. Su, *et al.*, NIR laser-triggered microneedle-based liquid band-aid for wound care, *Adv. Funct. Mater.*, 2021, **31**, 2100218.
31 L. Liu, X. Tian, Y. Ma, Y. Duan, X. Zhao and G. Pan, A versatile dynamic mussel-inspired biointerface: from specific cell behavior modulation to selective cell isolation, *Angew. Chem., Int. Ed.*, 2018, **57**, 7878–7882.
32 Y. Ma, X. Tian, L. Liu, J. Pan and G. Pan, Dynamic synthetic biointerfaces: from reversible chemical interactions to tunable biological effects, *Acc. Chem. Res.*, 2019, **52**, 1611–1622.
33 Y. Ma, P. He, W. Xie, Q. Zhang, W. Yin, J. Pan, M. Wang, X. Zhao and G. Pan, Dynamic colloidal photonic crystal hydrogels with self-recovery and injectability, *Research*, 2021, **2021**, 9565402.
34 Y. Zhang, M. Wu, D. Tan, Q. Liu, R. Xia, M. Chen, Y. Liu, L. Xue and Y. Lei, A dissolving and glucose-responsive insulin-releasing microneedle patch for type 1 diabetes therapy, *J. Mater. Chem. B*, 2021, **9**, 648–657.
35 Y. Zhang, J. Li, M. Wu, Z. Guo, D. Tan, X. Zhou, Y. Li, S. Liu, L. Xue and Y. Lei, Glucose-responsive gold nanocluster-loaded microneedle patch for type 1 diabetes therapy, *ACS Appl. Bio Mater.*, 2020, **3**, 8640–8649.
36 M. Wu, Y. Zhang, Q. Liu, H. Huang, X. Wang, Z. Shi, Y. Li, S. Liu, L. Xue and Y. Lei, A smart hydrogel system for visual detection of glucose, *Biosens. Bioelectron.*, 2019, **142**, 111547.
37 W. Schuurman, P. A. Levett, M. W. Pot, P. R. van Weeren, W. J. A. Dhert, D. W. Hutmacher, F. P. W. Melchels, T. J. Klein and J. Malda, Gelatin-methacrylamide hydrogels as potential biomaterials for fabrication of tissue-engineered cartilage constructs, *Macromol. Biosci.*, 2013, **13**, 551–561.
38 K. Yue, G. Trujillo-de Santiago, M. M. Alvarez, A. Tamayol, N. Annabi and A. Khademhosseini, Synthesis, properties, and biomedical applications of gelatin methacryloyl (GelMA) hydrogels, *Biomaterials*, 2015, **73**, 254–271.
39 Y. Piao, H. You, T. Xu, H.-P. Bei, I. Z. Piwko, Y. Y. Kwan and X. Zhao, Biomedical applications of gelatin methacryloyl hydrogels, *Engineered Regeneration*, 2021, **2**, 47–56.
40 A. Matsumoto, T. Ishii, J. Nishida, H. Matsumoto, K. Kataoka and Y. Miyahara, A synthetic approach toward a self-regulated insulin delivery system, *Angew. Chem., Int. Ed.*, 2012, **51**, 2124–2128.
41 P. I. Haris and F. Severcan, FTIR spectroscopic characterization of protein structure in aqueous and non-aqueous media, *J. Mol. Catal. B: Enzym.*, 1999, **7**, 207–221.
42 A. A. Aldana, L. Malatto, M. A. U. Rehman, A. R. Boccaccini and G. A. Abraham, Fabrication of Gelatin Methacrylate (GelMA) Scaffolds with Nano- and Micro-Topographical and Morphological Features, *Nanomaterials*, 2019, **9**, 120.
43 Y. Wada, Y. K. Yap, M. Yoshimura, Y. Mori and T. Sasaki, The control of BN and BC bonds in BCN films synthesized using pulsed laser deposition, *Diamond Relat. Mater.*, 2000, **9**, 620–624.
44 X. T. Fan, Z. X. Liu, J. G. Huang, D. Han, Z. H. Qiao, H. H. Liu, J. Du, H. Yan, Y. Y. Ma and C. Y. Zhang, *et al.*, Synthesis, curing mechanism, thermal stability, and surface properties of fluorinated polybenzoxazines for coating applications, *Adv. Compos. Hybrid Mater.*, 2022, **5**, 322–334.
45 N. A. Bakh, A. B. Cortinas, M. A. Weiss, R. S. Langer, D. G. Anderson, Z. Gu, S. Dutta and M. S. Strano, Glucose-responsive insulin by molecular and physical design, *Nat. Chem.*, 2017, **9**, 937–944.
46 S. Mura, J. Nicolas and P. Couvreur, Stimuli-responsive nanocarriers for drug delivery, *Nat. Mater.*, 2013, **12**, 991–1003.

47 C. Zhang, M. D. Losego and P. V. Braun, Hydrogel-based glucose sensors: Effects of phenylboronic acid chemical structure on response, *Chem. Mater.*, 2013, **25**, 3239–3250.
48 A. K. Yetisen, N. Jiang, A. Fallahi, Y. Montelongo, G. U. Ruiz-Esparza, A. Tamayol, Y. S. Zhang, I. Mahmood, S. A. Yang and K. S. Kim, *et al.*, Glucose-sensitive hydrogel optical fibers functionalized with phenylboronic acid, *Adv. Mater.*, 2017, **29**, 1606380.
49 M. Elsherif, M. U. Hassan, A. K. Yetisen and H. Butt, Glucose sensing with phenylboronic acid functionalized hydrogel-based optical diffusers, *ACS Nano*, 2018, **12**, 2283–2291.
50 B. Xue, J. Gu, L. Li, W. Yu, S. Yin, M. Qin, Q. Jiang, W. Wang and Y. Cao, Hydrogel tapes for fault-tolerant strong wet adhesion, *Nat. Commun.*, 2021, **12**, 7156.
51 K. Zheng, Q. Gu, D. Zhou, M. Zhou and L. Zhang, Recent progress in surgical adhesives for biomedical applications, *Smart Mater. Med.*, 2022, **3**, 41–65.
52 F. Meng, Q. Liu, Z. Shi, D. Tan, B. Yang, X. Wang, K. Shi, M. Kappl, Y. Lei and S. Liu, *et al.*, Tree frog-inspired structured hydrogel adhesive with regulated liquid, *Adv. Mater. Interfaces*, 2021, **8**, 2100528.
53 Q. Liu, D. Tan, F. Meng, B. Yang, Z. Shi, X. Wang, Q. Li, C. Nie, S. Liu and L. Xue, Adhesion enhancement of micropillar array by combining the adhesive design from gecko and tree frog, *Small*, 2021, **17**, 2005493.
54 K. Gelse, E. Pöschl and T. Aigner, Collagens—structure, function, and biosynthesis, *Adv. Drug Delivery Rev.*, 2003, **55**, 1531–1546.
55 S. L. Wong, M. Demers, K. Martinod, M. Gallant, Y. Wang, A. B. Goldfine, C. R. Kahn and D. D. Wagner, Diabetes primes neutrophils to undergo NETosis, which impairs wound healing, *Nat. Med.*, 2015, **21**, 815–819.
56 T. Yu, M. Gao, P. Yang, Q. Pei, D. Liu, D. Wang, X. Zhang and Y. Liu, Topical insulin accelerates cutaneous wound healing in insulin-resistant diabetic rats, *Am. J. Transl. Res.*, 2017, **9**, 4682–4693.
57 P. Yang, X. Wang, D. Wang, Y. Shi, M. Zhang, T. Yu, D. Liu, M. Gao, X. Zhang and Y. Liu, Topical insulin application accelerates diabetic wound healing by promoting anti-inflammatory macrophage polarization, *J. Cell Sci.*, 2020, **133**, jcs235838.
58 H. Brem and M. Tomic-Canic, Cellular and molecular basis of wound healing in diabetes, *J. Clin. Invest.*, 2007, **117**, 1219–1222.
59 X. Wang, D. Tan, X. Zhang, Y. Lei and L. Xue, Effective elastic modulus of structured adhesives: from biology to biomimetics, *Biomimetics*, 2017, **2**, 10.